U.S. DEPARTMENT OF THE INTERIOR
U.S. GEOLOGICAL SURVEY

Prepared for the
NATIONAL AERONAUTICS AND SPACE ADMINISTRATION

ATLAS OF VENUS
1:5,000,000 GEOLOGIC SERIES
GALINDO QUADRANGLE—VENUS
(V-40) I-2613
Pamphlet accompanies map

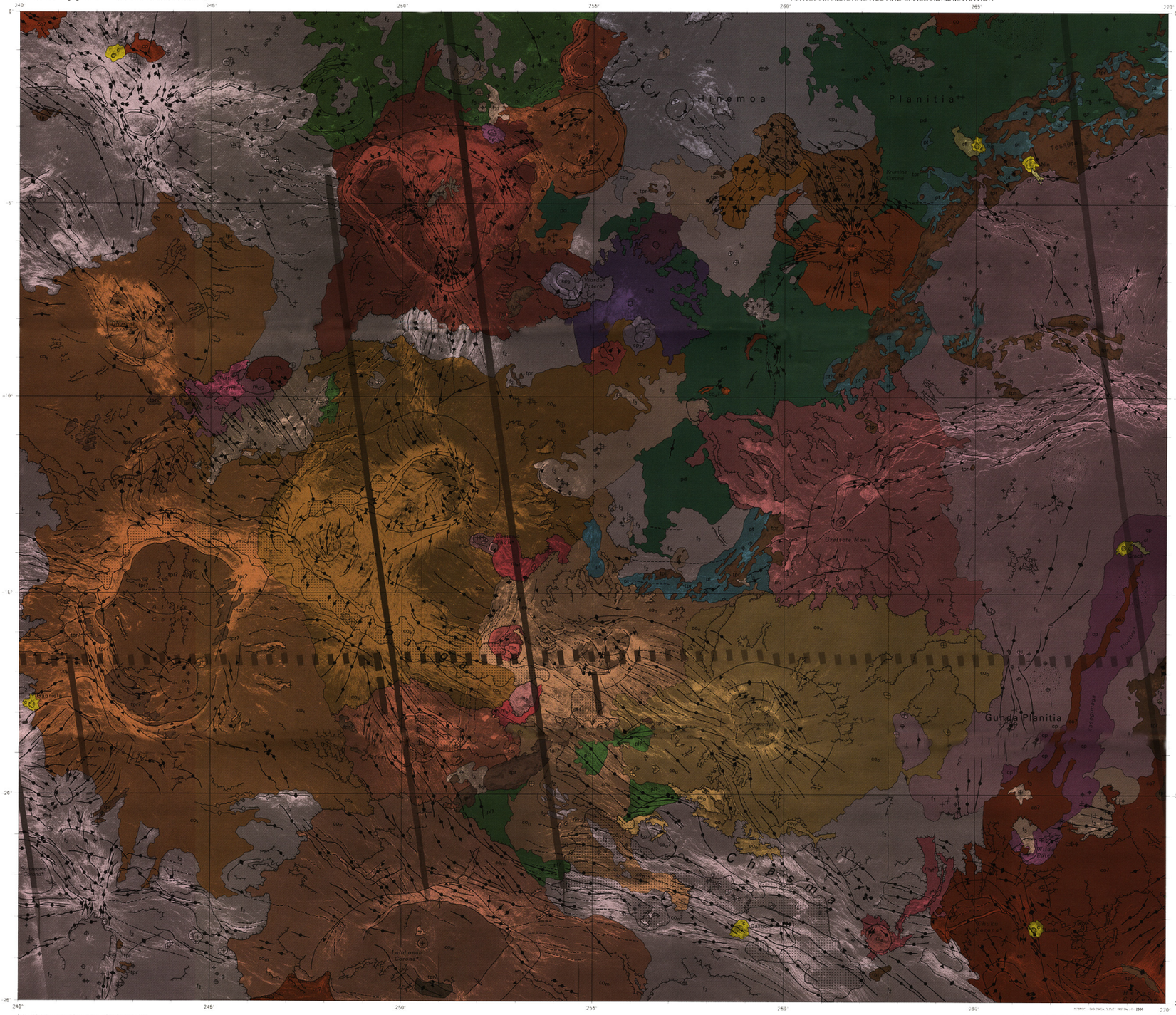

* Asterisk indicates provisional name, which has not been approved by the International Astronomical Union

SCALE 1:5 198 981 (1 cm = 51.96 km) AT 0° LATITUDE
1:2 771 366 AT 25° LATITUDE
MERCATOR PROJECTION

Prepared on behalf of the Planetary Geology Program, Solar System Exploration Division, Office of Space Science, National Aeronautics and Space Administration

Edited by Denise D. Hixson, cartography by Michael E. Bryant
Manuscript approved for publication August 26, 1997

QUADRANGLE LOCATION

Photomosaic location is shown in the western hemisphere of Venus. An outline of 15,000,000-scale quadrangles is provided for reference.

CORRELATION OF MAP UNITS

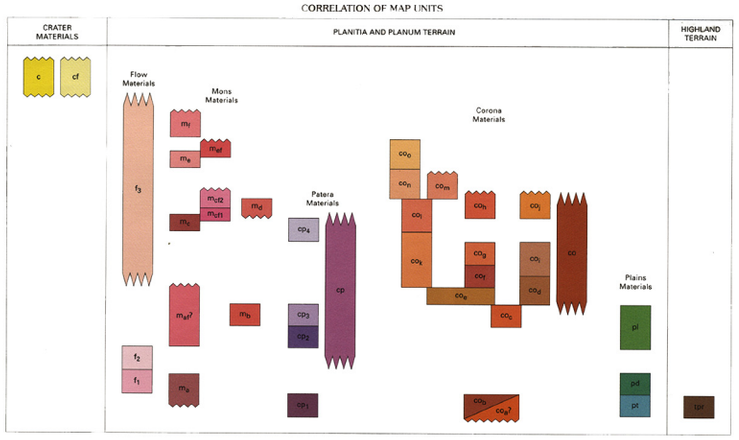

DESCRIPTION OF MAP UNITS

[Descriptions of material units from SAR images of Magellan data reflect surface scattering properties, varying with polarization, incidence angle of transmitted radar waves, surface roughness, and surface physical-electric properties. Therefore, unit descriptions of relative brightness do not translate to those seen in other planetary surface images acquired in the visible wavelengths. Relative ages for units established by stratigraphic relations; the cumulative densities of craters are too low on Venus for dating at the 1:5,000,000 scale. Topographic measurements approximated from 500-m contour map (fig. 1B). Radar correlation and quantitative surface properties available for some units (fig. 9, table 1).]

CRATER MATERIALS

c **Crater material**—Material of radar-bright, bowl-shaped craters having complete rim crests, steep walls, ejecta (soil) preserved and in all cases superposed on other materials. Some craters may have flat radar-dark floors; some craters may be deformed by subsequent fracturing. *Interpretation:* Young impact craters; impact melt present on some crater floors

cf **Outflow deposit**—Radar-bright, digitate lobes trailing away from ejecta of impact craters. *Interpretation:* Impact-melt flows

PLANITIA AND PLANUM TERRAINS

Flow materials—Consist of outcrops of varied radar reflectance, locally bound by lobate edges and containing numerous, scattered small tholi. Average surface properties quantified on figure 8. *Interpretation:* Volcanic flows and associated small cones

f_3 **Unit 3**—Occurs locally in patches superposed on material units as old as corona unit e and flow unit 2

f_2 **Unit 2**—Occurs over much of the map area underlying coronae units c to; shows one embayment relation with flow unit 1 at lat 20.5° S., long 264.5°

f_1 **Unit 1**—Embays Phoebe Regio tessera material and tessera-embaying plains material on east part of map area. Overlain by flow unit 2 and other mons, corona, and patera units

Mons materials—Consist of interdigitate tongues of varied radar reflectance bound by lobate edges that can be traced to cone- or dome-shaped mountains. *Interpretation:* Flank and radial lavas associated with and corresponding shield volcanoes

m_f **Unit f**—Traceable to 2-km-high cone (at 13° S., long 262°) containing central pit. Flows embay Phoebe Regio tessera material and corona units a and o

m_{ef} **Unit e flow material**—Relatively radar bright lobate flows traceable to two cone-shaped mounds mapped as unit e. Superposed on corona units e, l, and n

m_e **Unit e**—Occurs on two cone-shaped mounds near center of map area; having heights between 0.5 and 2 km. Superposed on corona units e, l, and n

m_d **Unit d**—Forms a fractured, 1-km-high mound at lat 16° S., long 253°; embayed by corona material n

m_{cf2} **Unit c flow material 2**—Radar-dark material traceable up the slope of a 1.5-km-high mound (unit mc) at lat 9° S., long 247°; superposed on unit c flow material 1 and corona material k

m_{cf1} **Unit c flow material 1**—Radar-bright lobate flows traceable up the slope of a 1.5-km-high mound (unit mc) at lat 9° S., long 247°; superposed on corona material k

m_c **Unit c**—Forms a 1.5-km-high, mound at lat 9° S., long 247° with a central crater; superposed on flow unit 2

m_b **Unit b**—Forms 500-m-high mound at lat 9° S., long 255.5°; includes adjacent small crater. Embayed by corona unit e and overlies patera unit 2

m_{af}? **Unit a flow material**—Radar-bright, lobate flows traceable to 500-m-high mound on southeast corner of map area; overlies flow unit 2 and, in places, undivided corona material

m_a **Unit a**—On southeast corner of map area, radar bright 500-m-high mound cut by radial and concentric graben; embayed by flow unit 2

Patera materials—Interdigitate tongues of material having varied radar reflectance and bound by lobate edges surrounding shallow, single-rim craters. *Interpretation:* Lava flows erupted from volcano-tectonic caldera depressions

cp_4 **Unit 4**—Relatively radar-bright material and radar-dark flows traceable to 500-m-deep crater at lat 9° S., long 257°. Associated flows embay corona units d, g, and i; overlain by corona units h and j

cp_3 **Unit 3**—Occurs on and around two craters near lat 8° S., long 255°. Superposed on unit 2; overlain by corona units e and f

cp_2 **Unit 2**—Relatively radar-bright lobate material associated with crater 20 km wide and 500 m deep at lat 7.5° S., long 256°. Overlies material of unit 1 and flow unit 2

cp_1 **Unit 1**—Material surrounding crater 30 km wide and 500 m deep at lat 6.5° S., long 256°. Overlain by radar-dark plains material

cp **Patera material, undivided**—Relatively radar-bright material traceable to 1-km-deep crater in southeast part of map area; overlain by radar-dark corona material, undivided

Corona materials—Digitate lobes of varied radar reflectance traceable to material fractured in roughly circular, ring pattern; some materials are deformed into outer trenches or moats. Discerned characteristics include width between bounding annular fractures or rings, shape of rings, number of rings, and topography (change in elevation between rings). *Interpretation:* Lavas emitted from coronae, arachnoids, and some of volcano-tectonic origin likely related to upwelling of mantle plume material

co_o **Unit o**—Material forming a 160-km-diameter, concentric, multiple ring, 500-m-high mound (at 18.5° S., long 259.5°); overlies material of corona unit n

co_n **Unit n**—Material forming a 150-km-diameter, slightly asymmetric, single ring, 1.5-km-high mound (at 16.5° S., long 258.5°); overlies material of corona units e and l

co_m **Unit m**—Material forming a 400-km-diameter, asymmetric, single ring, 1.5-km-high mesa (at 24° S., long 251°); overlies material of corona unit l; may contain embayed kapukas of radar-bright, ridged terrain (unit tpr?)

co_l **Unit l**—Material forming a 160-km-diameter, concentric, double ring depression of 1.5 km between annuli (at 19° S., long 250°); overlies corona units e and k

co_k **Unit k**—Interbedded materials forming a 450-km-diameter, asymmetric, partial double ring, mostly 1-km-high mesa (at 16° S., long 244°) and about a 200-km-diameter, concentric, radially fractured, 500-m-high mound (at 8° S., long 243°). Overlies corona unit e; may contain embayed kapukas of radar-bright, ridged terrain (unit tpr?)

co_j **Unit j**—Material forming a 70-km-diameter, concentric ring depression of 500 m (at 4.5° S., long 259°); overlies material of corona unit i and patera unit 4

co_i **Unit i**—Material forming a 70-km-diameter, concentric, 500-m-high ring (at 3° S., long 260°); overlies corona unit d

co_h **Unit h**—Material forming a 100-km-diameter, concentric, partial double ring depression of 1 km (at 1.5° S., long 255°); overlies corona unit g and patera unit 4

co_g **Unit g**—Material forming a 200-km-diameter, concentric, 500-m-high rim (at 3° S., long 254.5°); overlies corona unit f

co_f **Unit f**—Material forming a 500-km-diameter, asymmetric, partial double ring, mostly 1-km-high mesa, Jastre Corona (at 5° S., long 251°). Overlies material of corona unit e

co_e **Unit e**—Material forming a 525-km-diameter, asymmetric, single ring, radially fractured, 1- to 2-km-high mesa (at 12.5° S., long 250°); overlies flow unit 2

co_d **Unit d**—Material forming a 140-km-diameter, asymmetric, slightly elevated double ringed mound (at 4° S., long 261.5°); overlies corona unit c

co_c **Unit c**—Material forming a 70-km-diameter, concentric, single ring, 1-km-high mound (at 6° S., long 261.7°). Underlies material of corona unit d and overlies older plains materials

co_b **Unit b**—Forms material of partially buried single ring of an apparent 70-km-diameter, concentric, shallow depression (at 8.5° S., long 259°). Underlies radar-dark plains material and cut by north-trending fractures

co_a? **Unit a**—Forms material of largely buried, possible ring of an approximate 70-km-diameter, concentric, 500-m depression (at 9.8° S., long 258°). Southeast of, buried more than, and having a depression deeper than corona unit b. Underlies radar-dark plains material

co **Corona material, undivided**—Outcrops as lobate flows of varied radar reflectance about several coronae; three se mostly off map area. Overlies plains material; may contain embayed kapukas of radar-bright, ridged terrain (unit tpr?)

Plains materials—Indiscriminate plains differing only in relative radar reflectance and stratigraphic age. Average surface properties quantified in table 1. *Interpretation:* Lava flood deposits

pl **Radar-light plains material**—Forms plains in northern part of map area having a relatively light or radar bright appearance. Underlies flow unit 2, superposed by corona units f–o

pd **Radar-dark plains material**—Forms plains of relatively radar dark appearance. Embays corona units a? and b, Phoebe Regio tessera material, and tessera embaying plains material

pt **Tessera-embaying plains material**—Forms plains that embay tessera material. Superposed by radar-dark plains material and flow units 1 and 2

HIGHLAND TERRAIN MATERIAL

t **Tessera material of Phoebe Regio**—Occurs on topographic highs 0.5 to 2 km of Phoebe Regio and southern hills (were hills separated from the regio by graben fields). Material forms closely spaced, relatively radar bright ridges and lineations having variable widths and lengths averaging 1 to 10 km apart. Occurs with secondary perpendicular ridge set having spacing of 1 to 30 km. Overlain by other material types in map area. *Interpretation:* Oldest unit in map area; consists of complex ridged terrain material (Bindschadler and Head, 1991); some isolated hills may have been tilted from Phoebe Regio

Contact—Dashed where approximately located, queried where uncertain

Lobate front—Ticks point downslope; dashed where approximately located. Interpreted as a lava or impact-crater flow front

Narrow channel—Arrows point in direction of flow. Interpreted as lava channel

Linear scarp—Line marks top of scarp, barbs point downslope

Graben—Many are schematic and representative of numerous unmapped features

Lineament—Radar-bright linear feature of undiscernible morphology. Interpreted as a fracture

Ridge—Fairly wide (>5 km), symmetric highs, extending several tens to hundreds of kilometers. Many are schematic and representative of numerous unmapped features

Wrinkle ridge—Narrow, sinuous highs having asymmetric profiles

Corona annulus ridge—Somewhat concentric, asymmetric ridge following trend of annulus rings; shows axial trace and plunge. Short arrow indicates steeper limb or scarp bounding corona trough

Corona trough—Barbs point to trough axis

Large cone—More than 25 km diameter. Interpreted as volcanic shield

Small depression—Depth ≤2 km; some interpreted as calderas

Large depression—Depth greater than or equal to 2 km. Most form part of Parga Chasma

Splotch—Circular, radar-bright halo on surface. Interpreted as result of unknown surface changes due to atmospheric shock waves from impacting body

Small tholi—Conical hill, diameter 50 to 5 km. Interpreted as small volcanic edifice; size of circle indicates size and shape of cone

Impact crater—Shows rim; lobate deposit denotes impact melt outflow

Nova

The Magellan Mission

The Magellan spacecraft orbited Venus from August 10, 1990, until it plunged into the Venusian atmosphere on October 12, 1994. Magellan had the objectives of (1) improving knowledge of the geologic processes, surface properties, and geologic history of Venus by analysis of surface radar characteristics, topography, and morphology and (2) improving knowledge of the geophysics of Venus by analysis of Venusian gravity.

The Magellan spacecraft carried a 12.6-cm radar system to map the surface of Venus. The transmitter and receiver systems were used to collect three datasets: synthetic aperture radar (SAR) images of the surface, passive microwave thermal emission observations, and measurements of the backscattered power at small angles of incidence, which were processed to yield altimetric data. Radar emission and altimetric and radiometric measures of the Venusian surface were done in mission cycles 1, 2, and 3, from September 1990 until September 1992. Ninety-eight percent of the surface was mapped with radar resolution of approximately 120 meters. The SAR observations were projected to a 75-m nominal horizontal resolution; these full-resolution data compose the image base used in geologic mapping. The primary polarization mode was horizontal transmit, horizontal-receive (HH), but additional data for selected areas were collected for the vertical polarization sense. Incidence angles varied from about 20° to 45°.

High-resolution Doppler tracking of the spacecraft was done from September 1992 through October 1994 (mission cycles 4, 5, 6). High-resolution gravity observations from about 950 orbits were obtained between September 1992 and May 1993, while Magellan was in an elliptical orbit with a periapsis near 175 kilometers and an apoapsis near 8,000 kilometers. Observations from an additional 1,500 orbits were obtained following orbit-circularization in mid-1993. These data exist as a 75° by 75° harmonic field.

Magellan Radar Data

Radar backscatter power is determined by the morphology of the surface at a broad range of scales and by the intrinsic reflectivity, or dielectric constant, of the material. Topography at scales of several meters and larger can produce quasi-specular echoes, with the strength of the return greatest when the local surface is perpendicular to the incident beam. This type of scattering is most important at very small angles of incidence, because natural surfaces generally have few large tilted facets at high angles. The exception is in areas of steep slopes, such as ridges or rift zones, where favorably tilted terrain can produce very bright signatures in the radar image. For most other areas, diffuse echoes from roughness at scales comparable to the radar wavelength are responsible for variations in the SAR return. In either case, the echo strength is also modulated by the reflectivity of the surface material. The density of the upper few wavelengths of the surface can have a significant effect. Low-density layers, such as crater ejecta or volcanic ash, can absorb the incident energy and produce a lower observed echo. On Venus, a rapid increase in reflectivity exists at a certain critical elevation, above which high dielectric minerals or coatings are thermodynamically stable. This effect leads to very bright SAR echoes from virtually all areas above that critical elevation.

The measurements of passive thermal emission from Venus, though of much lower spatial resolution than the SAR data, are more sensitive to changes in the dielectric constant of the surface than to roughness. As such, they can be used to augment studies of the surface and to discriminate between roughness and reflectivity effects. Observations of the near-nadir backscatter power, collected using a separate smaller antenna on the spacecraft, were modeled using the Hagfors expression for echoes from gently undulating surfaces to yield estimates of planetary radius, Fresnel reflectivity, and root-mean-square (rms) slope. The topography data produced by this technique have horizontal footprint sizes of about 10 km near periapsis and a vertical resolution of approximately 100 m. The Fresnel reflectivity data provide a comparison to the emissivity maps, and the rms slope parameter is an indicator of the surface tilts, which contribute to the quasi-specular scattering component.

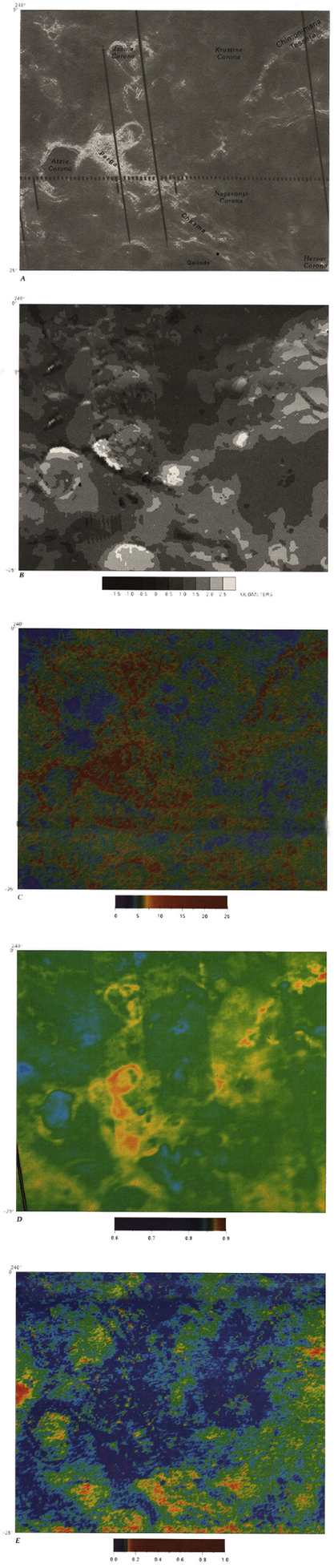

Figure 1. Magellan datasets for the Galindo quadrangle; north is toward top, quadrangle is approximately 3,300 km wide. ***A.*** Synthetic aperture radar backscatter mosaic generated from left-looking images stored to compare with ***B*** *–****E***, contains geographic names. ***B.*** Altimetry shows depth of Parga Chasma and heights of Phoebe Regio and volcanic features. ***C.*** Root mean square (rms) slope shows highly fractured terrains having rms slopes ≥20 degrees. ***D.*** Emissivity shows rough areas and low dielectric content materials to have higher (brighter) values. ***E.*** Reflectivity shows efficiency of surface materials in reflecting electron radiation. Most plains units having a reflectivity of about 0.1 shown as blue.

GEOLOGIC/GEOMORPHIC MAP OF THE GALINDO QUADRANGLE (V–40), VENUS

By
Mary G. Chapman

1999

ISBN 0-607-93986-9

For sale by U.S. Geological Survey, Information Services
Box 25286, Federal Center, Denver, CO 80225